

Milliwatt second harmonic generation in quantum cascade lasers with modal phase matching

O. Malis, A. Belyanin, D.L. Sivco, J. Chen, A.M. Sergent, C. Gmachl and A.Y. Cho

Milliwatt second harmonic power at 4.45 μm was achieved in InP lattice-matched quantum cascade lasers with monolithically-integrated resonant nonlinear cascades and modal phase matching. The use of an InP top-cladding layer and high-reflectance coating on the laser back facet enabled high linear laser power and consequently record nonlinear power.

Introduction: Nonlinear light generation has the potential of expanding the functionality of quantum cascade lasers (QCLs). In particular second harmonic (SH) generation has shown promise for extending the spectral range of QCLs beyond the limits imposed by the properties of the materials of choice [1, 2]. The mid-infrared range between 3 and 5 μm is of great importance for applications in high resolution *in situ* and remote trace gas sensing [3, 4]. SH generation in QCLs based on the well developed InP material system offers an alternative to other more technologically demanding lasers available in this spectral range.

Second harmonic generation: We are focusing on exploiting the properties of monolithically integrated resonant nonlinear cascades to enhance the nonlinear response of QCLs [1, 4]. This technique has proven promising for extending the operating wavelength of InP lattice-matched QCLs below 5 μm [5, 6]. The samples used in this study employ the fairly optimised InGaAs/InAlAs active region shown in Fig. 1b of reference [5]. In this case the QCL active region simultaneously acts as a source for the pump laser power and the nonlinear mixing region. The maximum nonlinear susceptibility for this active region is $|\chi^{(2)}| \sim 4 \times 10^{-5}$ esu (2×10^4 pm/V), assuming exact resonance for all interacting fields.

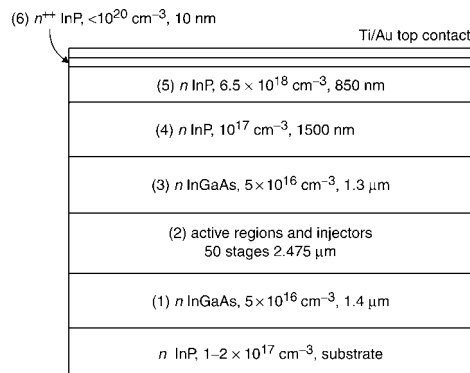


Fig. 1 Structure of InP-based waveguide optimised for phase matching (sample D3014)

The calculated refractive indices of the fundamental TM_{00} and SH TM_{02} modes for an infinitely wide waveguide are 3.2079 and 3.1689, respectively

Modal phase matching: A necessary condition for efficient SH generation is phase-matching. We have shown previously that, owing to the flexibility in the design of the QCL waveguide, modal phase matching is possible for these devices [6]. In contrast to other phase matching techniques, such as birefringent matching, or quasi-phase matching, modal phase matching allows for the exact matching of the effective refractive indices of transversal modes of different order. Moreover, unlike other techniques proposed for asymmetric double quantum wells [7, 8], modal phase matching is compatible with the intrinsic waveguide dispersion, weak voltage tunability, and strict current transport requirements of QCLs. In the case of second harmonic generation the best results are obtained by matching the refractive indices of the fundamental TM_{00} mode and SH TM_{02} mode. In this study we designed a waveguide that employs InP for both the top and the bottom (substrate) claddings. InP offers the advantage of better confinement and lower optical losses at both wavelengths of interest. The thicknesses of the waveguide layers are detailed in Fig. 1 and were chosen to reach the phase matching between the fundamental TM_{00} and SH TM_{02} modes for the waveguide ridge width of

7.3 μm . The difference between the effective refractive indices of the fundamental and SH modes depends quite strongly on the waveguide ridge width: the phase mismatch is $\Delta k = 538 \text{ cm}^{-1}$ for an infinitely wide waveguide. This dependence is used here to provide the tuning to exact phase matching by varying the ridge width.

Device fabrication: The QC laser structures used in this study (sample D3014) were grown by molecular beam epitaxy (MBE) on InP substrates in two steps. First, layers 1–3 were grown and the structure was capped with an As layer. Then the wafer was transferred to a second MBE machine equipped with a solid phosphorus source and top layers 4–6 were deposited. The devices were processed into 5–12 μm wide, 0.5–1.5 mm long deep-etched ridge-waveguide lasers [5]. The laser device back facets were high-reflectance (HR) coated, starting at the semiconductor, with SiO_2 2500 \AA /Ti 160 \AA /Au 1000 \AA / SiO_2 1000 \AA (reflectivity >99%). The last SiO_2 layer prevents In from creeping up the facet and shorting the device during soldering to the copper mounts.

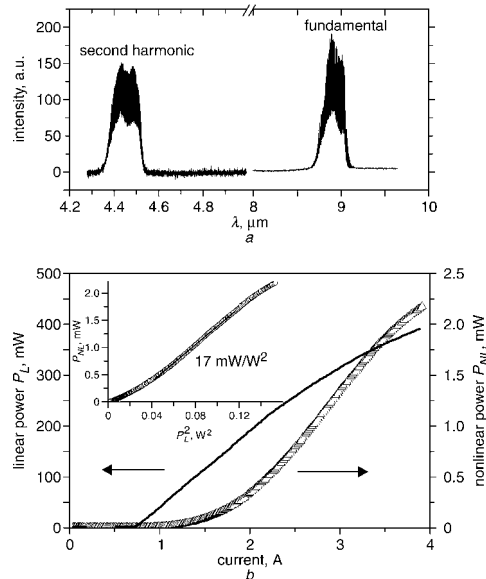


Fig. 2 Fundamental and second harmonic spectra, and light output power against current characteristics for sample D3014

Inset: SH power against linear power squared. The fit of the curve with a straight line in the central region gives the nonlinear conversion efficiency a Fundamental and second harmonic spectra for a 7 μm -wide, 1.5 mm-long laser with waveguide structure shown in Fig. 1 and HR-coating on back facet b Fundamental (solid) and SH (triangles) light output power against current characteristics at 10 K for sample in a

Device characteristics: The samples were characterised using a temperature-controlled He cryostat. All measurements discussed in this Letter were taken at cryogenic temperatures, around 10 K. The lasers were operated in pulsed mode with 50–100 ns current pulse widths at repetition rates of 4 and 84.2 kHz. The laser emits around 8.9 μm and the second harmonic signal was measured around 4.45 μm . The high resolution spectra shown in Fig. 2a were taken with a cooled HgCdTe (MCT) detector for the fundamental and a cooled InSb detector for the second harmonic. The laser radiation was attenuated with a metal filter to avoid detector saturation, while the second harmonic measurements were taken with a sapphire window and a quartz filter to eliminate the laser radiation. The SH far-field radiation pattern was found to have two unequal maxima located symmetrically with respect to the waveguide axis at angles of approximately 35° from the normal to the laser facet in a plane perpendicular to the device layers. This is consistent with the expected far-field distribution for the TM_{02} mode. The light output against current ($L-I$) measurements of the maximum propagating above the waveguide were taken with a calibrated fast uncooled MCT photovoltaic detector for the fundamental light, and a calibrated, cooled InSb detector for the SH light. Devices with ridge widths between 5 and 12 μm were characterised and the optimal width was found to be around 7 μm . Fig. 2b shows the $L-I$ curves at the fundamental and SH wavelengths for a 7 μm wide, 1.5 mm-long laser with the waveguide structure shown in Fig. 1. The laser displays a record maximum nonlinear power of 2 mW, and a nonlinear efficiency (slope of inset of Fig. 2b) of

approximately 17 mW/W². The accuracy of the InSb detector calibration was checked by measuring the same $L-I$ curve with the room temperature MCT detector and a sapphire filter to block the laser power (not shown here). The nonlinear efficiency is lower but comparable with the highest nonlinear conversion efficiency of 36 mW/W² reported previously [6]. Both measured values of the nonlinear efficiency are, however, considerably lower than the theoretical prediction of 2 W/W². The difference between the experimental values and the theoretical prediction is partially due to the 0.5 μm ridge width non-uniformity intrinsic to our wet-chemical mesa etching process. Deviation by 0.5 μm from the optimal ridge width would lead to the mismatch increase to $\Delta k \sim 50 \text{ cm}^{-1}$, and a decrease of the nonlinear efficiency by a factor of 7. The nonlinear power could be improved further by better control of the device dimensions using dry-etching mesa definition. Moreover, the theoretical calculations most likely underestimate the non-resonant losses and completely neglect the resonant losses at the SH frequency. Some of the common causes of higher experimental non-resonant losses in the mid-infrared are higher effective free carrier absorption and scattering owing to interface roughness in the MBE-growth material and on the ridge sides.

The superior performance of the devices based on the D3014 waveguide is due mainly to significantly improved laser characteristics reflected in lower threshold current ($J_{\text{th}} = 6.4 \text{ kA/cm}^2$ compared to 7.4 kA/cm^2 in our previous work) and higher maximum peak power (390 mW at 3.9 A compared to 290 mW at 3.3 A in our previous work). The HR coatings do not influence the nonlinear efficiency directly, but contribute to the improved laser performance by reducing the mirror losses that are reflected directly in the lower laser threshold current and higher slope efficiency. The HR coatings also allow laser operation at higher currents compared to devices without coatings. The narrower optimal ridge width (7 μm as opposed to 9 μm in the previous study [6]) is also beneficial because it suppresses the turn on of higher order in-plane transversal laser modes that are not phase matched to the SH modes.

Conclusions: Improvement by one order of magnitude in the power of second harmonic generation from InGaAs/InAlAs QCLs has been achieved by using an optimised InP waveguide for phase matching and HR-coatings for maximum laser power output. Reaching the milliwatt power range is significant as such a power level is sufficient for trace gas point sensors using mid-infrared light sources. The modal phase matching technique used in this work has proven promising for practical SH applications and can be generalised to other nonlinear light generation processes.

Acknowledgment: A.B. acknowledges support from the TAMU TITF Initiative and the ONR.

© IEE 2004

17 September 2004

Electronics Letters online no: 20047040

doi: 10.1049/el:20047040

O. Malis, D.L. Sivco, J. Chen, A.M. Sergent and A.Y. Cho (*Bell Laboratories, Lucent Technologies, 600 Mountain Ave., Murray Hill, NJ 07974, USA*)

E-mail: malis@lucent.com

A. Belyanin (*Department of Physics, Texas A&M University, College Station, TX 77843, USA*)

C. Gmachl (*Department of Electrical Engineering and PRISM, Princeton University, Princeton, NJ 08544, USA*)

References

- 1 Owschimikow, N., *et al.*: 'Resonant second-order nonlinear optical processes in quantum cascade lasers', *Phys. Rev. Lett.*, 2003, **90**, (4), pp. 0439021–0439024
- 2 Bengloan, J.-Y., *et al.*: 'Intracavity sum-frequency generation in GaAs quantum cascade lasers', *Appl. Phys. Lett.*, 2004, **84**, (12), pp. 2019–2021
- 3 Kosterev, A.A., and Tittel, F.K.: 'Chemical sensors based on quantum cascade lasers', *IEEE J. Quantum Electron.*, 2002, **38**, (6), pp. 582–591
- 4 Gmachl, C., *et al.*: 'Recent progress in quantum cascade lasers', *Reports Prog. Phys.*, 2001, **64**, pp. 1533–1601
- 5 Gmachl, C., *et al.*: 'Optimized second-harmonic generation in quantum cascade lasers', *IEEE J. Quantum Electron.*, 2003, **39**, (11), pp. 1345–1355
- 6 Malis, O., *et al.*: 'Improvement of second-harmonic generation in quantum cascade lasers with true phase matching', *Appl. Phys. Lett.*, 2004, **84**, (15), pp. 2721–2723
- 7 Meyer, J.R., *et al.*: 'Intersubband second-harmonic generation with voltage-controlled phase matching', *Appl. Phys. Lett.*, 1995, **67**, (5), pp. 608–610
- 8 Vodopyanov, K.L., *et al.*: 'Phase-matched second-harmonic generation in asymmetric double quantum wells', *Appl. Phys. Lett.*, 1998, **72**, (21), pp. 2654–2656